

Cellular brain edema induced by water intoxication in rat experimental model

Petr KOZLER, Dana MAREŠOVÁ, Jaroslav POKORNÝ

Institute of Physiology, First Faculty of Medicine, Charles University, Prague, Czech Republic

Correspondence to: Prof. MUDr. Jaroslav Pokorný, DrSc
Institute of Physiology, First Faculty of Medicine, Charles University
Albertov 5, Prague 2, 128 00, Czech Republic.
TEL: +420224968416; E-MAIL: jaroslav.pokorny@lfl.cuni.cz

Submitted: 2018-05-04 *Accepted:* 2018-06-02 *Published online:* 2018-09-15

Key words: **cellular brain edema; water intoxication; blood-brain barrier; brain water content; CT density; intracranial pressure; axonal impairment; locomotor activity**

Neuroendocrinol Lett 2018; **39**(3):209–218 PMID: 30431738 NEL390318A02 © 2018 Neuroendocrinology Letters • www.nel.edu

Abstract

OBJECTIVES: This paper presents our own rat model of the cellular brain edema, induced by water intoxication (WI). The basic principle of the model is an osmotic imbalance in the cell membrane followed by an intracellular flow of sodium and simultaneous accumulation of water leading to the subsequent increase of BBB permeability.

METHODS: The usefulness of the model was tested in precisely specified conditions whose results were clearly expressed. The procedure determined both how WI induces cellular edema as well as the disturbances caused by cellular edema.

RESULTS: The evidence of existing cellular edema with increased BBB permeability was proved by intracellular accumulation of intravital dye with a large molecular size; increased brain-water content was confirmed by using the dry/wet weight method and by the decrease in CT density; the elevated intracranial pressure (ICP) due to the expanding volume was determined by continuous monitoring the ICP; the structural lesions were proved by identification of the myelin disintegration; and the impaired nervous functions was demonstrated by the of open field test method.

CONCLUSION: Our experimental model can help the future studies of pathophysiology of cellular brain edema and is suitable for testing neuroprotective agents.

Abbreviations:

CE - Cellular edema
CNS - Central nervous system
BBB - Blood Brain Barrier
ICP - Intracranial pressure
WI - Water intoxication
TBI - Traumatic brain injury
SIADH - Syndrome of inappropriate antidiuretic hormone secretion
Da - Dalton
EB - Evans blue
MW - Molecular weigh
ICA - Internal carotid artery

CCA - Common carotid artery
ECA - External carotid artery
GD - Gyrus dentatus
IDI EB - Intracellular Distribution Index of EB
HH - hyperhydrated
ROI - regions of interest
MV HU - mean values of Hounsfield Units
SEM - standard error of the mean
i.p. - intraperitoneally
DW - distil water
deg C - degrees Celsius
AQP - aquaporin
ADH - antidiuretic hormone

INTRODUCTION

Edema can result from almost any insult to the brain, including trauma, infarction, neoplasm, or abscess, as well as conditions such as hypoxia, or toxic or metabolic perturbation. The present classification of edema doesn't replace Klatzo's classification (1967); it just extends it and makes it more specific (see Table 1).

In edema expanding volume causes increasing pressure with intracranial hypertension as a result. This life-threatening condition gives rise to high rates of mortality in such clinical pathologies, such as stroke and traumatic brain injury, where there's no causal management known at present. The prevailing cause of intracranial hypertension in both above-mentioned pathologies is cellular edema (Ayata & Ropper 2002; Kimelberg 1995; Kimelberg 2004; Liang *et al.* 2007; Marmarou 2007; Rhoney & Parker 2006). That is why we have long been studying the pathophysiology of cellular edema by means of a rat model, where edema is induced by water intoxication (Kozler *et al.* 2017a; Kozler *et al.* 2017b; Kozler & Pokorný 2014; Kozler & Pokorný 2012; Kozler & Pokorný 2003; Kozler *et al.* 2013; Marešová *et al.* 2014). In this paper we present methods and results of our experimental model in total.

At the beginning we briefly present some of the general pathophysiological principles representing the background of the model.

Water intoxication reduces the amount of solutes in the extracellular compartment due to their marked dilution and causes hyposmolality, with plasma hyponatremia being its constant factor. This creates an osmotic gradient that activates water movement from the extracellular space into the cells. Accumulation of water in cells triggers a cascade of events that leads to the failure of cellular metabolism and to the development of cytotoxic edema (Go 1997; Kimlberg 1995; Klatzo 1967). A recent view on the pathophysiology of cytotoxic edema was described by Liang *et al.* (2007). Cytotoxic edema (synonyms: cellular edema, oncotic cell swelling or oncosis) is a premorbid cellular process; its primary attribute is an influx and intracellular accumulation of extracellular Na⁺ and other cations into neurons and astrocytes. The influx of cations leads to the influx of anions in order to maintain electroneutrality, and the combination of these phenomena controls the influx of water into the cells. Water passes membrane through

specific water channels – aquaporins (AQP). In the movement of water in the CNS and for the formation of cellular edema, AQP4 plays an essential role (Agre *et al.* 2004; Hsu *et al.* 2015; Manley *et al.* 2000; Papadopoulos & Verkman 2007; Pasantes-Morales *et al.* 2002; Wells 1998). Cytotoxic edema itself does not lead to brain swelling, but it depletes the extracellular space for Na⁺, Cl⁻ and water, creating a new gradient for the flow of those ions and water from the capillaries of the gliovascular complex (Blood Brain Barrier, BBB). Specifically, this primary impact sets off a cascade of processes leading to a subsequent increase in BBB permeability. The cascade includes: a loss of calcium and potassium homeostasis (Barzó *et al.* 1997; Kimlberg 1995; Siesjo 1993), release of excitotoxic amino acids (Barzó *et al.* 1997; Bullock *et al.* 1994; Kimlberg 1995), release of free oxygen radicals (Barzó *et al.* 1997; Kimlberg 1995; Kontos 1989), and induction of intracerebral tissue acidosis (Barzó *et al.* 1997; Kimlberg 1995; Siesjo *et al.* 1993). Loss of selective permeability of the BBB leads to formation of the process known as brain edema, which is characterized by increased water content and volume of the brain (Klatzo 1967).

For the experimental model, adult male rats of the Wistar strain were used (weight 350–450 g, unless otherwise stated) and treated in accordance with the current Guidelines for the Treatment of Laboratory Animals (EU Guidelines 86/609/EEC). All experiments were approved by the Ethical Committee of the First Faculty of Medicine (Charles University in Prague).

Cellular edema was induced by water intoxication by injecting distilled water (DW) in a total amount corresponding to 20% of body weight intraperitoneally (i.p.) in three consecutive doses over 24 hours with a simultaneous administration of desmopressin. Each sub-dose represented one-third of the total dose of 0.032 mg/kg (desmopressin (1-desamino-8-D-arginine vasopressin) (OCTOSTIM[®], Ferring). Desmopressin is an antidiuretic hormone which potentiates the effect of hyperhydration by inducing hyponatremia (Manley *et al.* 2000; Silver *et al.* 1999; Yamaguchi *et al.* 1997; www.rxmed.com/b.main/b2.pharmaceutical/OCTOSTIM.html).

The results of all measurements were statistically evaluated using the GraphPad Prism 6 program (parametric ANOVA and nonparametric Kruskal-Wallis test; statistical significance was set at 5%), unless otherwise stated.

Tab. 1. Present classification of brain edema – modified according to Kimlberg (1995, 2004) and Marmarou (2007).

criteria	edema type	
pathogenesis	increased BBB permeability “vasogenic”	disturbed cell metabolism “cytotoxic”
accumulated water	extracellular	intracellular
extent	focal	diffuse
clinical pathology	tumor, abscess, hematoma, TBI (focal)	stroke, TBI (diffuse), SIADH, water intoxication

Legend: TBI = traumatic brain injury, SIADH = syndrome of inappropriate antidiuretic hormone secretion

The Materials and Methods, Results and Discussion sections are integral to the issues that were under study. Each issue is presented in a separate section.

ALTERED BLOOD BRAIN BARRIER PERMEABILITY

BBB permeability can be tested by different methods. The most widely used one in experimental models is the use of intravital dyes (tracers, markers) with a molecular weight greater than 180 Da precluding passage across an intact BBB. In terms of molecular size, these markers represent a broad spectrum of dyes, in which Evans blue (EB, MW 961 Da) is one of the largest. In blood circulation, it becomes strongly, though reversibly, bound to the albumin fraction of proteins to give rise to a high-molecular complex (EBA 68 500 Da) which cannot pass an intact BBB. (Broman 1944; Kroll & Neuwelt 1998; Lafuente *et al.* 1990; Pokorný *et al.* 2002; Wolman *et al.* 1981). In experimental models designed to test BBB permeability, EB is injected intravenously. In such experiments, EB presence in the brain is detected either macroscopically, using an all-brain staining scale, or microscopically, where evidence of EB permeation of the BBB is seen in its extravasation or in its presence in the brain capillary system. The purpose of our study was to obtain a histological picture of the propagation of Evans blue in hippocampal areas and its intracellular and extracellular distribution. For this purpose EB is applied into the carotid system (Greenwood *et al.* 1988; Saris *et al.* 1988).

Materials and methods

EB was injected into the right internal carotid artery (ICA) of hydrated rats (see method of water intoxication). For general anesthesia, each rat received 4 mg/100 g of thiopental applied intraperitoneally. Using a conventional technique, the right-sided common carotid artery (CCA), ICA and external carotid artery (ECA) were exposed from a linear incision between the sternal manubrium and mandible. A polyethylene catheter fixed by ligation was introduced into the bifurcation through a small arteriotomy of the CCA. The ECA ligated close behind the bifurcation. 2% EB at a dose of 2 ml/kg, was applied at a rate of 0.45 ml/min (Saris *et al.* 1988). Thirty min after the end of intracarotid injection, the brain was fixed by transcardial perfusion with a 4% paraformaldehyde solution in a pH 7.4 phosphate buffer 15 minutes, and then fixed in the same solution for another 24 hours. Each brain was then sliced on a vibratome into coronary sections 30 µm thick and then, without further staining, placed on slides for microscopic examination. The sections were studied under a fluorescence microscope for staining intensity and intracellular/extracellular distribution of EB in the CA1, CA3 areas, and in the hippocampal gyrus dentatus (GD) – both in the ipsilateral (right) and in the contralateral (left) hemispheres.

To rate the staining intensity, a three-degree scale of 1 to 3 (1 = faint, 2 = medium, 3 = intense) was used. Using the fluorescence microscope software “LUCIA Image Analysis System” the ratio of intracellular/extracellular distribution of EB in each estimated area was expressed by means of Intracellular Distribution Index of EB (IDI EB). IDI EB represents a precisely defined quantity from 0 to 2.0, where IDI EB = 1 means equal distribution of EB between the intracellular and extracellular compartments, IDI EB >1 shows more EB in the cells than in the extracellular compartment, IDI EB <1 exhibits most of the EB remaining outside the cells. As plasma natremia reflects the degree of water intoxication, hyponatremia confirms osmotic cellular edema. The respective blood samples were obtained from a catheter in the CCA before any of the applications.

This method was used in two groups of rats with three animals in each one – Group 1 (G1) with intact rats, Group 2 (G2) with rats after WI. The results represent the average of all the data obtained in three rats of each group.

Results

While the staining intensity was equal in both groups of animals reaching grade 1, there were significant differences in IDI EB between both groups (see Figure 1).

Fluorescence microscopy discovered noticeable differences of EB distribution. While in Group 1 a small amount of the marker was dispersed only in the extracellular compartment, in Group 2, the accumulated EB was visible in neuronal populations with a typical shape in the studied areas of the hippocampus (for an example, see Figure 2 for the differences in the CA1 area)

Plasma natremia in rats of Group 2 was, on average, 20 mmol/l lower than that in rats of Group 1 reflecting sufficient degree of water intoxication.

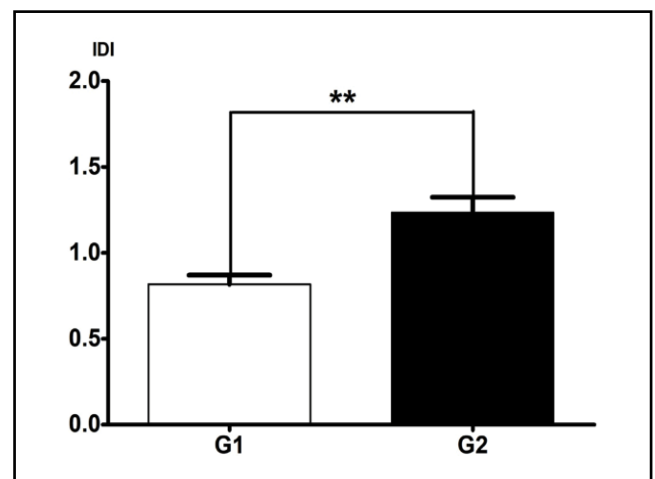


Fig. 1. Intracellular distribution index of Evans blue. Y axis: IDI quantity from 0.0 to 2.0, X axis: G1 = intact rats, G2 = rats after WI, **= $p < 0.01$

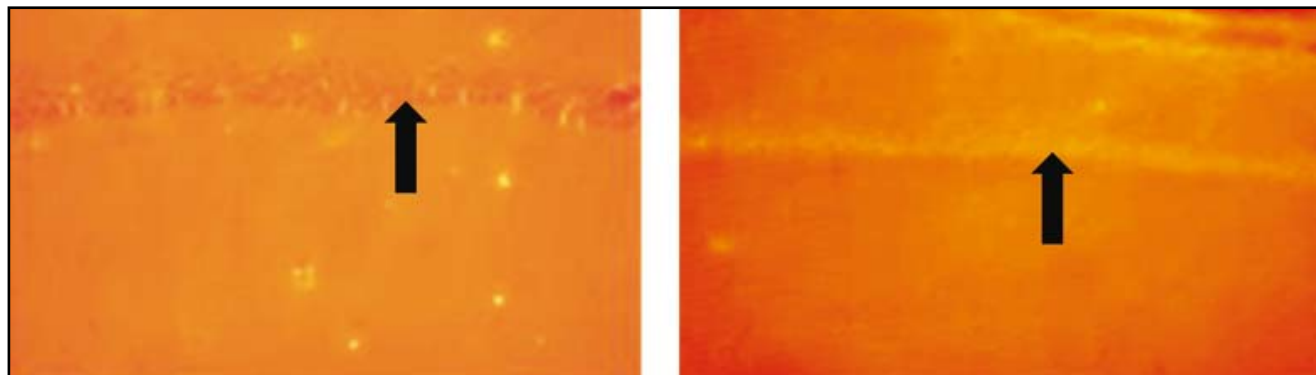


Fig. 2. Evans blue (EB) distribution in right CA1 area. Left: Group 1: EB dispersed in the extracellular compartment – high fluorescence of the neuropile, low fluorescence in CA1 neurons – red stripe (arrow); right: Group 2: EB accumulated intracellularly in CA1 neurons – yellow stripe (arrow).

Discussion

In rats of Group 1 (intact animals) the entry of the EB into the brain can be attributed to a number of factors which together influence the intact barrier on its luminal side. These concern a rapid increase in intravascular and, consequently, hydrostatic pressure (Barzó *et al.* 1997; Betz *et al.* 1989; Marshall *et al.* 1969), sudden hypervolemia in a limited area (Rapoport 2000), and lastly, the direct effect of the staining agent. The last resembles the side effect of an angiographic contrast medium (Broman & Olsson 1949). The staining intensity was faint and doesn't differ from the intensity in Group 2 with water intoxicated animals. Unlike this similarity, there were significant differences in IDI EB between both groups as well as documented differences of EB distribution in fluorescence microscopy. The results confirm the above-mentioned principle that cellular edema induced by WI brings about an osmotic imbalance at the cell membrane followed by an intracellular flow of sodium and simultaneous accumulation of

water leading to a subsequent increase of BBB permeability. Plasma hyponatremia as a constant factor of WI was confirmed (Kozler *et al.* 2003).

BRAIN WATER CONTENT

The aim of this issue was to determine whether changes induced by water intoxication are accompanied by increased brain-water content.

Materials and methods

There were two groups of rats in this experiment with six animals in each one – Group CG (control group with intact rats) and Group HH 20% (with rats after WI, where HH 20% means hyperhydrated animals with the total amount of water corresponding to 20% of body weight).

Rats were decapitated in a deep anesthesia (4 mg/100 g of thiopental applied intraperitoneally) and the brains were immediately removed, weighed (wet weight), placed in a thermostat at 86°C for a period of six days, and then weighed again (dry weight). The water content in the brain was determined in percentiles using the equation: $(\text{wet weight} - \text{dry weight}) / \text{wet weight} \times 100$ (Kamoun *et al.* 2009). The rats in Group HH 20% were decapitated eight hours after completing the WI.

Results

The water content was higher in the brains of the hyperhydrated animals (HH 20%) than in Group CG (see Figure 3).

Discussion

The results clearly show that water intoxication brings about a higher brain water content caused by cellular edema. The explanation for this phenomena corresponds to general pathophysiological principles creating the base of our model mentioned in the Introduction – water intoxication reduces the amount of solutes in the extracellular compartment due to their marked dilution and causes hypoosmolality, this creates an

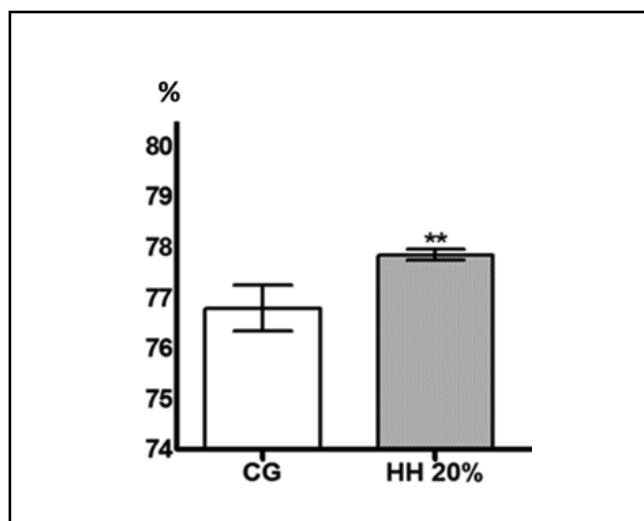


Fig. 3. Brain water content. Y axis: brain water content (%), X axis: CG: control group, HH 20%: experimental group, **= $p < 0.01$

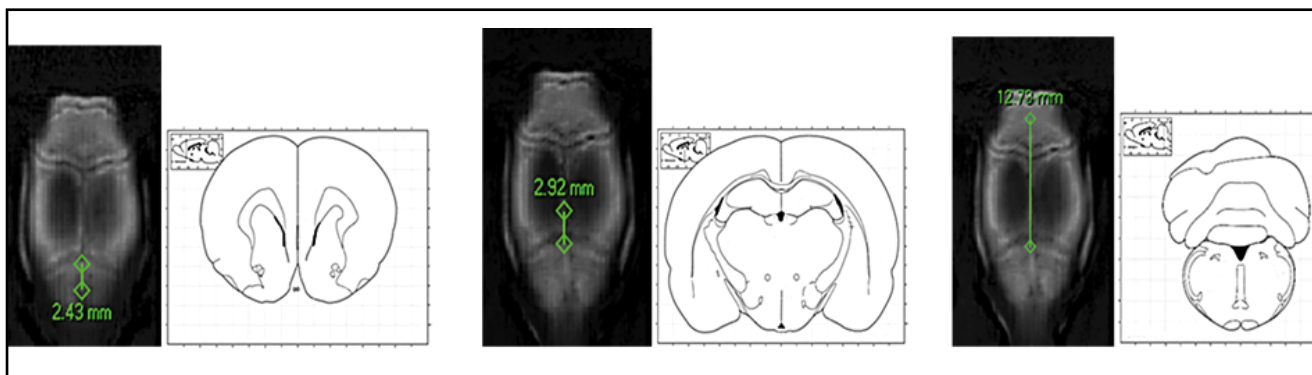


Fig. 4. Regions of interest (ROI) corresponding to the area of coronary sections (according to stereotactic atlas) with pixel size 0.125 mm in positions A, B, C. Right: position A: bregma +2.43 mm; middle: position B: bregma -2.92 mm; left: position C: bregma -12.73 mm.

osmotic gradient that activates the movement of water from the extracellular space into the cells. (Kimelberg 1995; Kimelberg 2004; Kozler *et al.* 2013).

CT DENSITY

The aim of this issue was to determine whether water intoxication affects the radiodensity of brain tissue in a CT scan.

Materials and methods

For the CT examination the Albira PET/CT system (Bruker, BioSpin, Spain) was used (in collaboration with the Institute of Physiology of the Czech Academy of Sciences).

Standard CT scans of the brain were obtained from a group of three rats, first under control conditions (CG Group – control group, intact animals) and then under experimental conditions (EG Group – edema group, rats after WI). The CT examination of the EG Group started 16 hours after finishing the WI. Scans with a pixel size 0.125 mm were done in regions of interest (ROI) corresponding to the area of coronary sections in three different positions, with bregma being the reference mark: position A (bregma +2.43 mm), position B (bregma -2.92 mm) and position C (bregma -12.73 mm) (see Figure 4).

Results

The CT density of the brain tissue in each scan was stated as mean values of Hounsfield Units (MV HU). After WI (EG Group) the brain density decreased (see Table 2).

The density differences shown in Table 2 were statistically significant in each position examined (see Figure 5).

Discussion

Under physiological conditions the CT density of the human brain is in the range of 29–38 HU (Kucinski *et al.* 2002; Mangal *et al.* 2002). If, under pathological

conditions, the density decreases at least by 12 HU, the radiological criterion for the presence of brain edema is fulfilled (Clasen *et al.* 1981; Torack 1982). The overall average density decrease in the edema group, as documented by our results, was 32.48 MV HU (see Table II.), high enough to conclude that rats after WI had brain edema. It must be stressed at this point, that the induced edema was a diffuse and cellular type, and the ROI comprised the entire coronary section of the brain (Kozler & Pokorny 2014). Due to a lack

Tab. 2. Density in Hounsfield Units (MV HU, mean values \pm standard deviation).

	CG Group	EG Group
density	120.49 \pm 5.7	88.01 \pm 3.36
density decrease		32.48

Legend: CG Group: control group, intact animals, EG Group – edema group, rats after WI, average: average MV HU in all three positions and in all animals.

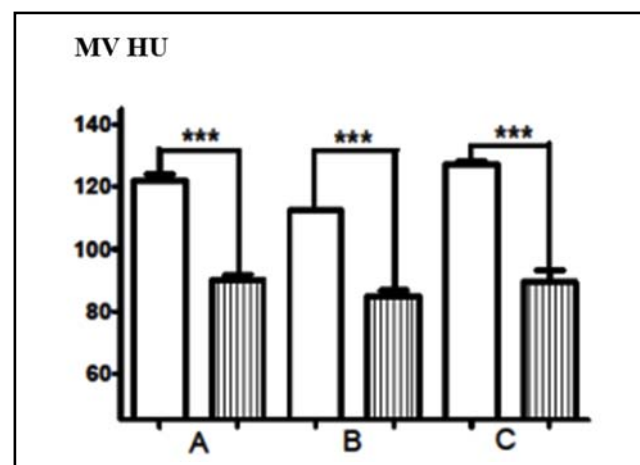


Fig. 5. Density of the brain in Hounsfield Units at positions A,B,C. Y axis: MV HU (mean values +SD), X axis: A,B,C: positions, empty columns: CG, striped columns: EG, ***= $p<0.001$

of valid information it is difficult to determine the CT density of a rat brain under physiological conditions as well as the density decrease denoting the presence of brain edema in rats. We found only one paper dealing with the experimental edema investigated by CT (Dzi-alowski *et al.* 2004) where normal density was 75.6 ± 2.2 HU with density drop of 3.9 HU after edema induction. The authors of this paper used a quite different experimental protocol – middle cerebral artery occlusion led to a focal type of brain edema, and the ROI areas were lesser, localized to the place of edema appearance only. That is why our results can't match the results of this study.

INTRACRANIAL PRESSURE

The aim of this issue was to determine whether water intoxication affects intracranial pressure. Continuous monitoring of the intracranial pressure (ICP) detects impending intracranial hypertension resulting from impaired intracranial volume homeostasis, when expanding volume generates an increase in pressure (Gupta 2015).

Materials and methods

A group of 16 animals was divided in the following groups of eight rats: C (control group, untreated animals), WI (animals with induced cellular edema).

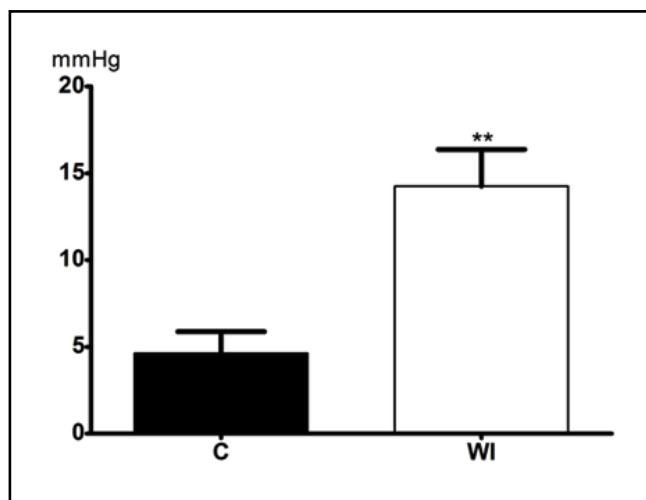


Fig. 6. Intracranial pressure values (mean \pm SEM). X axis: ICP in mmHg, Y axis: C – control group of intact rats, WI – rats with induced CE; **= $p < 0.01$

Continuous monitoring of intracranial pressure (ICP) using the fiber optic system OPSENS MEDICALÔ: spontaneously breathing rats under the inhalation anesthetic isoflurane (Forane®, AbbVie Ltd.) in a concentration of 2 volume % underwent, in the prone position, a longitudinal incision of the skin and subcutaneous tissue in the midline of the head; the freed galea aponeurotica was dissected, and the skull was trephined 3 mm laterally to the midline on the right and 3 mm frontally to the bregma; the dura was opened by incision and a microchip with a pressure sensor connected to a fiber optic transmitter was introduced intraparenchymally to a depth of 3 mm. The transmitter was wired to a digital monitor and pressure analyzer (using computer software) for continuous monitoring of the absolute values of ICP, with current ICP curves on the PC monitor. After monitoring for 60 minutes the microchip was removed, the durotomy and trepanopunction were sealed with Spongostan (SPONGOSTANÔ, Ferrosan), and the subcutaneous tissue and the scalp were sutured. Following completion of inhalation anesthesia, the rat spontaneously awoke from a side position after about 25–30 minutes (Murtha *et al.* 2012).

The IPC monitoring software evaluated an interval of 60 minutes for each animal (see Table 3 – results of one experimental animal).

Results

Mean ICP values (\pm SEM) of eight animals in both groups were as follows: C: 4.62 ± 1.24 , WI: 14.25 ± 2.12 , ICP values in the groups differed significantly (see Figure 6).

Discussion

In rats after WI, ICP values were significantly higher than those in the group of intact animals. As water intoxication increased the water content in the brain (Kozler & Pokorny 2014; Kozler *et al.* 2014), the measured values indicated the developing impairment of brain homeostasis. It can be concluded that cellular edema induced by WI leads to ICP elevation (Kozler *et al.* 2014).

AXONAL IMPAIRMENT

The aim of this issue was to determine whether cellular edema induced by water intoxication can lead to structural lesions. Based on a previously published study

Tab. 3. Example of 60-minute interval of ICP monitoring in one animal.

Unit	Minimum	Timestamp (s)	Maximum	Timestamp (s)	Mean	SEM
mmHg	2.2	10328	5.7	5396	4.308	0.6919

Legend: Minimum and Timestamp (s) – the lowest recorded ICP value and its duration in seconds; Maximum and Timestamp (s) – the highest recorded ICP value and its duration in seconds; Mean – average ICP value during 60 minutes of monitoring; SEM (standard error of the mean).

(Onaya 2002) we looked at the neurohistological pattern of myelin integrity.

Materials and methods

Perfusion and fixation. Animals were transcardially perfused in a deep anesthesia (4 mg/100 g of thiopental applied intraperitoneally) with a 4% solution of paraformaldehyde in 0.1 M phosphate buffer (pH 7.4) for 15 minutes. After removal from the skull, the brain was fixed in the same solution for 24 hours. Serial coronary sections (30- μ m thick) were sliced from each brain using a vibratome and placed on gelatin-coated slides and dried.

Neurohistology. The sections were rehydrated and axonal changes detected with the Black Gold II method of staining (Histo-Chem Inc., Jefferson, AZ, USA.) (Schmued & Slikker 1999). The hippocampal formation was the main part of the brain under study because of its known high sensitivity to various patho-

genic stimuli. Analysis was centered on the CA1 and CA3 areas of the hippocampus and on the dorsal blade of the dentate gyrus (DG).

The neurohistological picture of the structural integrity of the axons was assessed with the aid of the following grades of myelin degradation: 1 = no changes, 2 = sporadic oedematous vesicles and sporadic oedematous axons, 3 = multiple vesicles, varicosity, oedematous axons with helical or spiral course, 4 = myelin fragmentation (see Figure 7).

In this part of study three groups of rats with five animals in each one were used – Group CG (control group with intact rats), Group A1 (acute group – with rats after WI; the perfusion was done 30 minutes after completing the WI) and Group C1 (chronic group – with rats after WI, the perfusion was done 1 week after completing the WI).

Statistical analysis. The results were statistically evaluated using the t test and one-way analysis of vari-

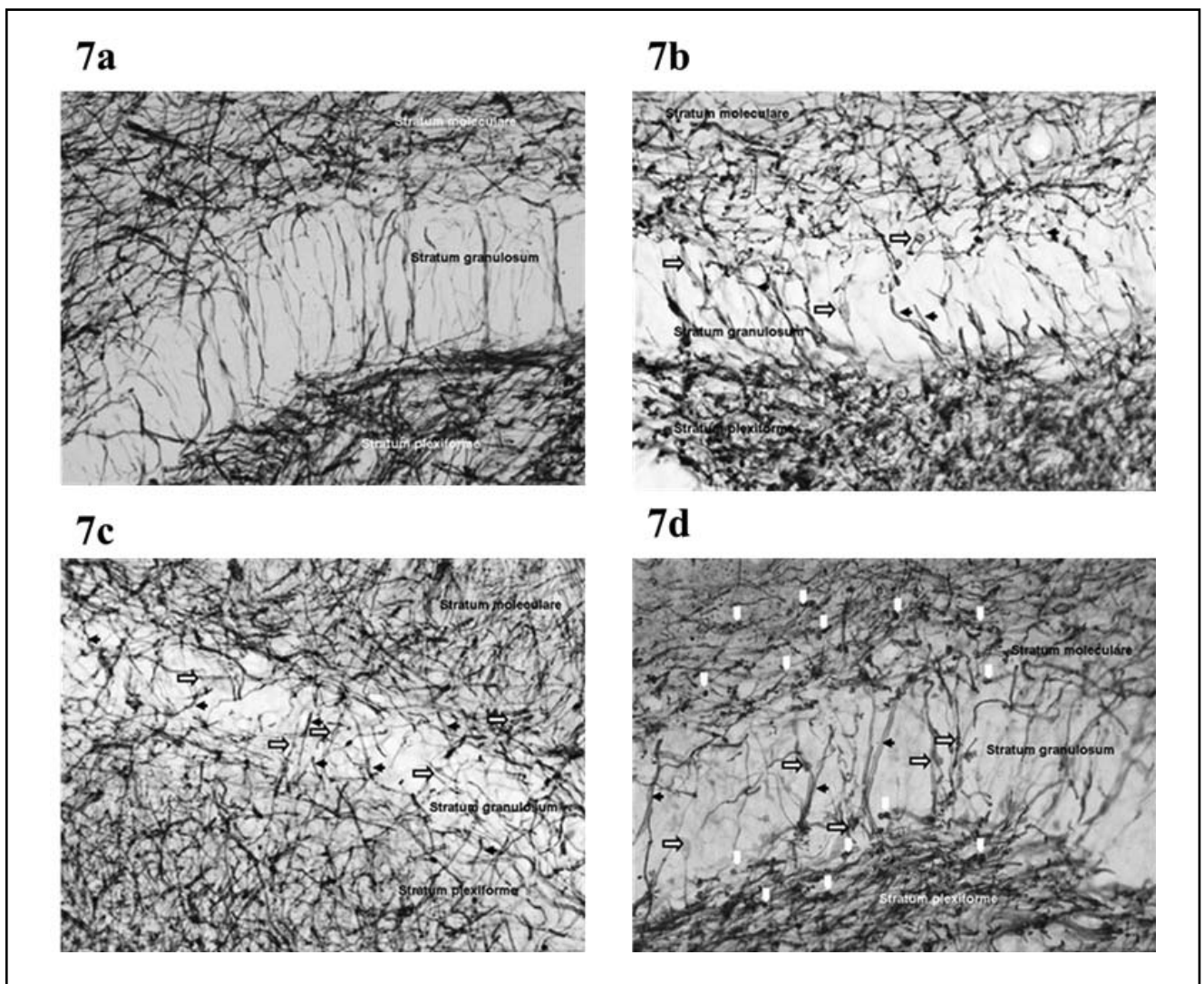


Fig. 7. Grades of myelin degradation. 7a: Gr.1 = No changes; 7b: Gr.2 = sporadic oedematous vesicles and sporadic oedematous axons (black arrows); 7c: Gr.3 = multiple vesicles, varicosity, oedematous axons and helical course of axons (white arrows); 7d: Gr.4 = myelin fragmentation (white columns).

ance (ANOVA) followed by a Dunnett post hoc analysis. The statistical software GraphPad Prism version 4.00 for Windows (GraphPad Software, San Diego, CA, USA) was used.

Results

The results confirmed structural lesions (disintegration of the myelin) due to cellular edema induced by WI. The disintegration was time dependant with more severe grades found in the chronic Group C1 (see Figure 8).

Discussion

Based on the neuropathological findings, Onaya (2002) determined that in diffuse axonal injuries the cellular edema always came before the disintegration of the axons. He concluded that the existence of diffuse axonal injuries without prior cellular edema is impossible. This postulate was confirmed by others (Creed *et al.* 2011; Stys 1998) including our own experience. The significant difference between the acute and chronic groups offers a therapeutic window for neuroprotection (Kozler & Pokorný 2012).

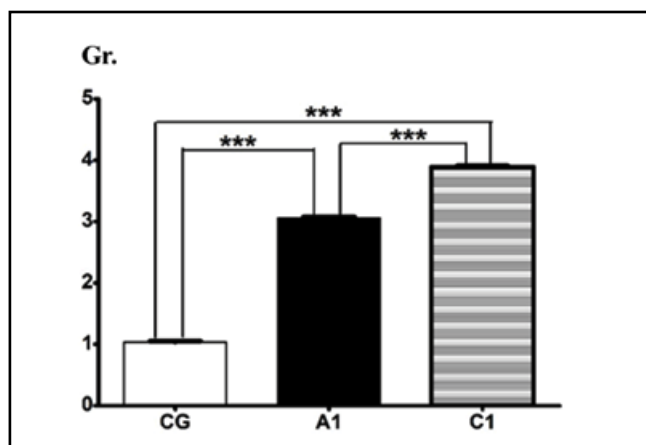


Fig. 8. Disintegration of the myelin. Y axis: grades of disintegration (see also Fig. 7), X axis: CG: control group, A1: acute group, C1: chronic group (see also section Materials and Methods), ***= $p < 0.001$

SPONTANEOUS LOCOMOTOR ACTIVITY

The aim of this issue was to determine if cellular brain edema induced by water intoxication affects spontaneous locomotor activity in adult rats.

Materials and methods

Rats were divided into groups of animals without water intoxication (Group A, 11 rats) and those that were water intoxicated (Group D, 8 rats). Locomotor activity (LA) of the rats was tested at an open field (Aragão *et al.* 2011; Hall 1934; Jandová *et al.* 2014; Russell *et al.* 2011; Slamberová *et al.* 2013).

Open field test. To test the locomotor activity of rats, we used the Laboras system (Metris, B.V., Netherland) for continuous registration and analysis of locomotor activity. The Laboras system consists of a triangular shaped sensing platform (carbon fiber plate 700 mm × 700 mm × 1000 mm × 30 mm), positioned on two orthogonally placed sensor-transducers and third fixed point attached to the bottom plate. A Makrolon polycarbonate cage (type III, 840 cm²) is placed on this platform. Any mechanical vibrations caused by the movement of the animal are converted into electrical signals, which are then evaluated using Laboras software. The animals were tested in a darkened room at a constant room temperature of 22 to 23 degrees C. Tests always took place at the same time, between 9:00 and 12:00, with 10 minutes of the testing recorded and analyzed each hour. The animals were tested for horizontal locomotor activity – average time spent in locomotion (s), average distance travelled (m) and average speed of locomotion (m/s).

Results

Average time spent in locomotion (s), average distance travelled (m) and average speed of locomotion (m/s) during one hour of rats after WI (Group D) were significantly suppressed, compared to the activity of the control rats (group A) (see Figure 9).

Discussion

The locomotor activity of rats with water intoxication (Group D – after WI) was lower than that in the control

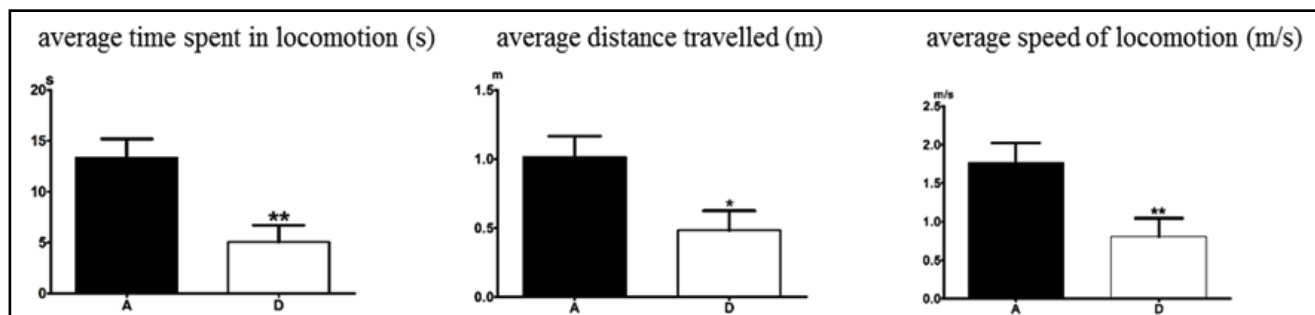


Fig. 9. Locomotor activity. Legend: horizontal axis A = without WI, D = after WI, vertical axis: locomotor activity in the studied categories: s = second, m = meter, m/s = meter /sec, *= $p < 0.05$, **= $p < 0.01$, ***= $p < 0.001$

rats (Group A) (see Figure 8). This decrease was caused by the induced cellular edema (Kozler *et al.* 2017a,b). Cellular edema in general reduces initiation and conduction of upper limb movements during locomotion, without functional or anatomical distress of the pathway that controls the movements (Inoue *et al.* 2013).

CONCLUSIONS

Each issue under study was targeted to a specific aim. The initial study analyzed the mechanism of how WI induces cellular edema with a subsequent increase of BBB permeability. Following studies analyzed the disturbances caused by cellular edema: Brain Water Content, CT Density and Intracranial Pressure determined impaired intracranial volume homeostasis, while Axonal Impairment determined structural damage, and Spontaneous Locomotor Activity and Neuronal Excitability determined functional changes.

The evidence of existing cellular edema with increased BBB permeability induced by WI was confirmed by a high Intracellular Distribution Index of Evans Blue (IDI EB >1 showing the presence of intravital dye with a large molecular size inside the cells) and by the accumulation of EB inside the neuronal population of the hippocampus (see Figures 1, 2).

The increase of the brain water content was measured by the dry/wet weight method and by a decrease in CT density (see Figures 3, 5). Continuous monitoring of ICP indicated elevated intracranial pressure due to the expanding volume (see Figure 6). These demonstrated results fulfil the basic criterion of the classification of brain edema established by Klatzo (1967): “an abnormal accumulation of fluid within the brain parenchyma and a volumetric enlargement of the tissue.”

The structural lesions were proved by the disintegration of the myelin, which was time dependant with more severe grades found after one week (see Figure 8). It must be underscored that no animal died and no animal became unconscious in this experiment. This supports the assumption that cellular edema induced in our model by WI is in its initial phase and could be still reversible despite the fact that it leads to structural lesions (Gennarelli & Graham 1998; Sahuquillo *et al.* 2001).

Applying the open field test (locomotor activity) confirmed impaired nervous functions (see Figure 9). Tested functions were attenuated due to cellular edema.

It can be concluded that in our model of cellular edema the conditions under study could be precisely specified and the obtained results could be clearly expressed – these are the basic features of an experimental model being suitable to test neuroprotective agents.

ACKNOWLEDGEMENTS

Supported by the grant PROGRES Q35/LF 1.

REFERENCES

- 1 Agre P, Nielsen S, Ottersen OP eds (2004). Brain Water Homeostasis. *Neuroscience*. **129**: 849–1054.
- 2 Aragão Rda S, Rodrigues MA, de Barros KM, Silva SR, Toscano AE, de Souza RE, Manhães-de-Castro R (2011). Automatic system for analysis of locomotor activity in rodents—a reproducibility study. *J Neurosci Methods*. **195**: 216–221.
- 3 Ayata C, Ropper AH (2002). Ischaemic brain oedema. *J Clin Neurosci*. **9**:113–124.
- 4 Barzó P, Marmarou A, Fatouros P, Hayasaki K, Corwin F (1997). Contribution of vasogenic and cellular edema to traumatic brain swelling measured by diffusion-weighted imaging. *J Neurosurg* **87**: 900–907.
- 5 Betz AL, Iannotti F, Hoff JT (1989). Brain edema: a classification based on blood-brain barrier integrity. *Cerebrovasc Brain Metab Rev*. **1**: 133–154.
- 6 Broman T, Olsson O (1949). Experimental study of contrast media for cerebral angiography with reference to possible injurious effects on the cerebral blood vessels. *Acta Radiol* **49**: 321–334.
- 7 Broman T (1944). Supravital analysis of disorders in the cerebral vascular permeability in man. *Acta Med Scand*. **118**: 79–83.
- 8 Bullock R, Zauner A, Tsuji O (1994). Excitatory amino acid release after severe human head trauma: effect of intracranial pressure and cerebral perfusion pressure changes. In: *Intracranial Pressure IX*. eds Nagai H, Kamiya K, Ishii S, Springer, Tokyo, pp 264–267.
- 9 Clasen RA, Huckman MS, Von Roenn KA, Pandolfi S, Laing I, Lobick JJ (1981). A correlative study of computed tomography and histology in human and experimental vasogenic cerebral edema. *J Comput Assist Tomogr*. **5**: 313–327.
- 10 Creed JA, DiLeonardi AM, Fox DP, Tessler AR, Raghupathi R (2011). Concussive brain trauma in the mouse results in acute cognitive deficits and sustained impairment of axonal function. *J Neurotrauma*. **28**: 547–563.
- 11 Dzialowski I, Weber J, Doerfler A, Forsting M, von Kummer R (2004). Brain tissue water uptake after middle cerebral artery occlusion assessed with CT. *J Neuroimaging*. **14**: 42–48.
- 12 Gennarelli TA, Graham DI (1998). Neuropathology of the head injuries. *Semin Clin Neuropsychiatry* **3**: 160–175.
- 13 Go KG (1997). The normal and pathological physiology of brain water. *Adv Tech Stand Neurosurg*. **23**: 47–142.
- 14 Greenwood J, Luther PJ, Pratt OE, Lantos PL (1988). Hyperosmolar opening of the blood-brain barrier in the energy-depleted rat brain. Part 1. Permeability studies. *J Cereb Blood Flow Metab*. **8**: 9–15.
- 15 Gupta G (2015). Intracranial pressure monitoring. <http://emedicine.medscape.com/article/1829950-overview>
- 16 Hall CS (1934). Emotional behavior in the rat. I. Defecation and urination as measures of individual differences in emotionality. *Journal of Comparative Psychology*. **18**: 385–403.
- 17 Hsu Y, Tran M, Linninger AA (2015). Dynamic regulation of aquaporin-4 water channels in neurological disorders. *Croat Med J*. **31**: 401–421.
- 18 Inoue T, Lin A, Ma X, McKenna SL, Creasey GH, Manley GT (2013). Combined SCI and TBI: recovery of forelimb function after unilateral cervical spinal cord injury (SCI) is retarded by contralateral traumatic brain injury (TBI), and ipsilateral TBI balances the effects of SCI on paw placement. *Exp Neurol*. **248**: 136–147.
- 19 Jandová K, Kozler P, Langmeier M, Marešová D, Pokorný J, Riljak V (2014). Influence of low-dose neonatal domoic acid on the spontaneous behavior of rats in early adulthood. *Physiol Res*. **63** Suppl 4: S521–528.
- 20 Kamoun WS, Ley CD, Farrar CT, Duyverman AM, Lahdenranta J, Lacorre DA, Batchelor TT, Di Tomaso E, Duda DG, Munn LL, Fukumura D, Sorensen AG, Jain RK (2009). Edema control by cediranib, a vascular endothelial growth factor receptor-targeted kinase inhibitor, prolongs survival despite persistent brain tumor growth in mice. *J Clin Oncol*. **20**: 2542–2552.
- 21 Kimelberg HK (1995). Current concepts of brain edema. Review of laboratory investigations. *J Neurosurg*. **83**:1051–1059.
- 22 Kimelberg HK (2004). Water homeostasis in the brain: basic concepts. *Neuroscience*. **129**: 851–860.

- 23 Klatzo I (1967). Presidential Address. Neuropathological aspects of brain edema. *J Neuropathol Exp Physiol.* **26**: 1–14.
- 24 Kontos HA (1989). Oxygen radicals in CNS damage. *Chem Biol Interact.* **72**: 229–255.
- 25 Kozler P, Marešová D, Pokorný J (2017a). An experimental model of the "dual diagnosis": Effect of cytotoxic brain edema plus peripheral neuropathy on the spontaneous locomotor activity of rats. *Neuro Endocrinol Lett.* **38**: 101–107.
- 26 Kozler P, Marešová D, Pokorný J (2017b): Methylprednisolone modulates intracranial pressure in the brain cellular edema induced by water intoxication. *Physiol Res* **66** Suppl. 4: S511–S516.
- 27 Kozler P, Pokorný J (2014). CT density decrease in water intoxication rat model of brain oedema. *Neuro Endocrinol Lett.* **35**: 608–612.
- 28 Kozler P, Pokorný J (2012). Effect of methylprednisolone on the axonal impairment accompanying cellular brain oedema induced by water intoxication in rats. *Neuro Endocrinol Lett.* **33**: 782–786.
- 29 Kozler P, Pokorný J (2003). Altered Blood-Brain Barrier Permeability and Its Effect on the Distribution of Evans Blue and Sodium Fluorescein in the Rat Brain Applied by Intracarotid Injection. *Physiol. Res.* **52**: 607–614.
- 30 Kozler P, Riljak V, Pokorný J (2013). Both Water Intoxication and Osmotic BBB Disruption Increase Brain Water Content in Rats. *Physiol. Res.* **62** Suppl. 1: S75–S80.
- 31 Kroll RA, Neuwelt EA (1998). Outwitting the blood-brain barrier for therapeutic purposes: osmotic opening and other means. *Neurosurgery* **42**: 1083–1100.
- 32 Kucinski T, Väterlein O, Glauche V, Fiehler J, Klotz E, Eckert B, Koch C, Röther J, Zeumer H (2002). Correlation of apparent diffusion coefficient and computed tomography density in acute ischemic stroke. *Stroke.* **33**: 1786–1791.
- 33 Lafuente JV, Pouschman E, Cervós-Navarro J, Sharma HS, Schreiner C, Korves M (1990). Dynamics of tracer distribution in radiation induced brain oedema in rats. *Acta Neurochir.* **51** Suppl: 375–377.
- 34 Liang D, Bhatta S, Gerzanich V, Simard JM (2007). Cytotoxic edema: mechanisms of pathological cell swelling. *Neurosurg Focus.* **15**: E2
- 35 Mangel L, Vönöczky K, Hanzély Z, Kiss T, Agoston P, Somogyi A, Németh G (2002). CT densitometry of the brain: a novel method for early detection and assessment of irradiation induced brain edema. *Neoplasma.* **49**: 237–242.
- 36 Manley GT, Fujimura M, Ma T, Noshita N, Filiz F, Bollen AW, Chan P, Verkman AS (2000). Aquaporin-4 deletion in mice reduces brain edema after acute water intoxication and ischemic stroke. *Nat Med.* **6**: 159–163.
- 37 Marmarou A (2007). A review of progress in understanding the pathophysiology and treatment of brain edema. *Neurosurg Focus.* **15**: E1.
- 38 Marshall WJS, Jackson JLF, Langfitt TW (1969). Brain swelling caused by trauma and arterial hypertension. *Arch Neurol.* **21**: 545–553.
- 39 Murtha L, McLeod D, Spratt N (2012). Epidural intracranial pressure measurement in rats using a fiber-optic pressure transducer. *J Vis Exp.* **25** pii: 3689.
- 40 Onaya M (2002). Neuropathological investigation of cerebral white matter lesions caused by closed head injury. *Neuropathology.* **22**: 243–251.
- 41 Papadopoulos MC, Verkman AS (2007). Aquaporin-4 and brain edema. *Pediatr Nephrol.* **22**: 778–784.
- 42 Pasantes-Morales H, Franco R, Ordaz B, Ochoa LD (2002). Mechanisms counteracting swelling in brain cells during hyponatremia. *Arch Med Res.* **33**: 237–244.
- 43 Pokorný J, Hrachovina V, Langmeier M, Trojan S (2002). Long-term changes of the blood brain barrier permeability from the view of reparation plasticity. *Physiol Res.* **51**: 35P
- 44 Rapoport SI (2000). Osmotic opening of the blood-brain barrier: principles, mechanism, and therapeutic applications. *Cell Moll Neurobiol.* **20**: 217–230.
- 45 Rhoney DH, Parker D, Jr (2006). Considerations in fluids and electrolytes after traumatic brain injury. *Nutr Clin Pract.* **21**: 462–478.
- 46 Russell KL, Kutchko KM, Fowler SC, Berman NE, Levant B (2011). Sensorimotor behavioural tests for use in a juvenile rat model of traumatic brain injury: assessment of sex differences. *J Neurosci Methods.* **199**: 214–222.
- 47 Sahuquillo J, Poca MA, Amorós S (2001). Current aspects of pathophysiology and cell dysfunction after severe head injury. *Curr Pharm Des.* **7**: 1475–1503.
- 48 Saris SC, Wright DC, Oldfield EH, Blasberg RC (1988). Intravascular streaming and variable delivery to brain following carotid artery infusions in the Sprague-Dawley rat. *J Cereb Blood Flow Metab.* **8**: 116–120.
- 49 Schmued L, Slikker W (1999). Black-gold; a simple, high-resolution histochemical label for normal and pathological myelin in brain tissue sections, *Brain Research.* **837**: 289–297.
- 50 Siesjo BK, Katsura K, Mellegard P (1993). Acidosis-related brain damage. *Prog Brain Res.* **96**: 23–48.
- 51 Siesjo BK (1993). Basic mechanisms of traumatic brain damage. *Ann Emerg Med.* **22**: 959–969.
- 52 Silver SM, Schroeder BM, Bernstein P, Sterns RH (1999). Brain adaptation to acute hyponatremia in young rats. *Am J Physiol.* **276**: R1595–1599.
- 53 Slamberová R, Macúchová E, Nohejlová-Deykun K, Schutová B, Hrubá L, Rokyta R (2013). Gender differences in the effect of prenatal methamphetamine exposure and challenge dose of other drugs on behaviour of adult rats. *Physiol Res.* **62** Suppl 1: S99–S108.
- 54 Stys PK (1998). Anoxic and ischemic injury of myelinated axons in CNS white matter: from mechanistic concepts to therapeutics. *J Cereb Blood Flow Metab.* **18**: 2–25.
- 55 Torack RM (1982). Computed tomography and stroke edema: case report with an analysis of water in acute infarction. *Comput Radiol.* **6**: 35–41.
- 56 Wells T (1998). Vesicular osmometers, vasopressin secretion and aquaporin-4: a new mechanism for osmoreception? *Mol Cell Endocrinol.* **15**: 103–107.
- 57 Wolman M, Klatzo I, Chui E, Wilmes F, Nishimoto K, Fujiwara K, Spatz M (1981). Evaluation of the dye-protein tracers in pathophysiology of the blood-brain barrier. *Acta Neuropathol.* **54**: 55–61.
- 58 www.rxmed.com/b.main/b2.pharmaceutical/OCTOSTIM.html
- 59 Yamaguchi M, Yamada T, Kinoshita I, Wu S, Nagashima T, Tamaki N (1997). Impaired learning of active avoidance in water-intoxicated rats. *Acta Neurochir Suppl.* **70**: 152–154.